Electronic Supplementary Material (ESI) for Journal of Materials Chemistry B.

Supporting Information

Dual-Environment-Sensitive Probe to Detect Proteome Aggregation in Stressed Laryngeal Carcinoma Cells and Tissues

Biao Jing[b, ‡], Yanjie Bi[a, ‡], Hui Kong [a], Wang Wan [b], Jizhe Wang [*a], Bo Yu [*a]

a. The Second Hospital of Dalian Medical University, 467 Zhongshan Road, Dalian, 116023, China.

b. Dalian Institute of Chemical Physics, Chinese Academy of Sciences, 457 Zhongshan Road, Dalian 116023, China.

‡. These authors contributed equally to this work

1. Experimental method

1.1 Synthetic Procedures

All synthesis followed literature reported methods.[1]

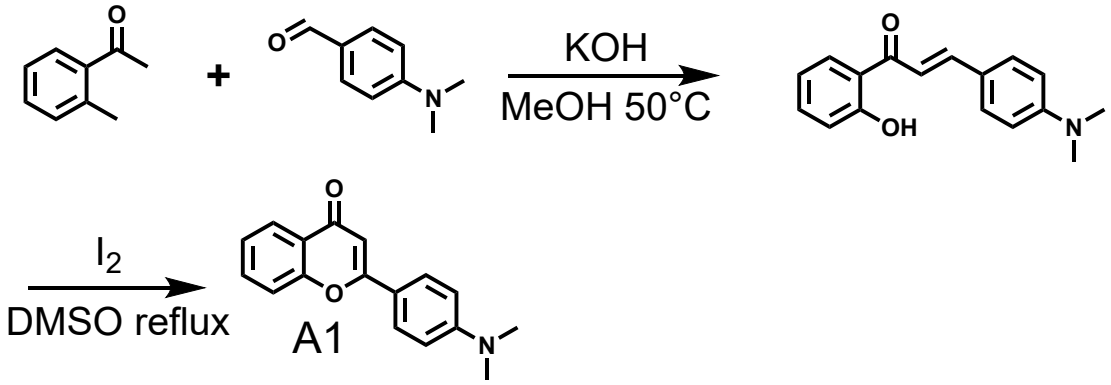

A1: Synthesis of P0, 2-(4-(dimethylamino) phenyl)-4H-chromen-4-one (**A1**):

KOH (8.40 g) was dissolved in anhydrous methanol (75 mL) at 0 °C, subsequently 2'-hydroxyacetophenone (5.4 mL, 45.0 mmol) and 4-dimethylamino-benzaldehyde (4.92 g, 33.0 mmol) were added. The reaction mixture was stirred and maintained at 50 °C for 48 h, then quenched with water, acidified to pH ≈ 6, and extracted against ethyl acetate. The organic layer was washed with saturated brine and dried over Na_2SO_4. 3-[4-(dimethylamino) phenyl]-1-(2-hydroxyphenyl)-2-propen-1-one was recrystallized from ethyl acetate to yield a dark-red crystal, and used without further purification. 3-[4-(dimethylamino) phenyl]-1-(2-hydroxyphenyl)-2-propen-1-one (1.07 g, 4.0 mmol) and I2 (16 mg, 0.04 mmol) were dissolved in 15 mL DMSO. The reaction mixture was refluxed for 1 h, and then cooled to room temperature. The reaction mixture was diluted with DCM, and then extra DMSO was removed by extraction with water. The crude **A1** was obtained after removed all solvent, and then purified through flash silica gel chromatography (PE/ EA = 1:1) to yield light-yellow solid. ^{1}HNMR (400 MHz, $CDCl_3$) δ 8.21 (dd, J = 8.0 Hz, 1H), 7.86 (d, J = 8.0 Hz, 2H), 7.67 (td, J = 8.0 Hz, 1.6 Hz, 1H), 7.54 (d, J = 8.0 Hz, 1H), 7.40 (t, J = 8.0 Hz, 1H), 6.90 (d, J = 8.0 Hz, 2H), 6.78 (s, 1H), 3.10 (s, 6H) ppm. ^{13}C-NMR (100 MHz, $CDCl_3$) δ 178.3, 162.5, 156.0, 139.9, 138.6, 133.4, 128.6, 125.6, 124.8, 124.2, 120.7, 117.7, 112.4, 109.4, 51.6, 40.4 ppm. HRMS (m/z) Anal. Calc'd for $C_{17}H_{15}NO_2$ $(M+H)^+$: 266.1176, Found $(M+H)^+$: 266.1177

1.2 Fluorescence spectra and solvatochromism measurement

To assess solvatochromism, A1 were initially prepared as a 1 mM stock solution in DMSO and subsequently diluted to a concentration of 20 μM using various solvents. For fluorescence measurement, 100 μL of each diluted sample was transferred into a BeyoGold 96-Well Black Opaque plate. The fluorescence intensity was then recorded using a Tecan Spark Fluorescence Plate Reader, with each spectrum being normalized to its highest fluorescence intensity for comparison.

1.3 Density functional theory (DFT) calculations

All the calculations of the single-molecule properties studied in this work were performed using the Gaussian16 program package.[2] After literature analysis and functional tests, a large number of research showed that the B3LYP functional can describe the electronic structure of the studied molecules very well. Therefore, the ground state and excited state of these studied molecules were respectively optimized by DFT//B3LYP/6–31G (d,p) and TDDFT//B3LYP/6–31G (d,p). Besides, the vibration frequency was further analyzed to ensure that the real local minima ware found without imaginary frequency, and the wave function stability of the optimized structure is tested to confirm the basis of our results is stable. We used the TDDFT//B3LYP/6–31G (d,p) method to calculate the excited state properties of molecule in vacuo, chlormethine, dioxane, methanol, water solutions.

1.4 Viscosity dependence measurement and calculation

To control the impact of solvent polarity on the fluorescence readings, a blend of glycerol and ethylene glycol was used. This choice was made because both liquids have closely matched dielectric constants—46.5 for glycerol and 37.0 for ethylene glycol—making them similarly polar. To create mixtures with varying viscosities, the volume fraction of glycerol in ethylene glycol was altered in increments: 0%, 20%, 40%, 60%, 80%, and 100%. The viscosity of these different mixtures was then determined based on a previously published method [3]. The equation S1 was used for calculating the mixture viscosity, given that the viscosity of glycerol is 1500 mPa·S and that of ethylene glycol is 25.66 mPa·S.

$$ln\eta_{m_{ix}} = \Sigma_{i=1}^{n} w_i \cdot \ln \eta_{mix} \quad \text{(S1)}$$

All samples were diluted from a 1 mM DMSO stock to a final concentration of 20 μM. Fluorescence emission readings were taken with a Tecan Spark Fluorescence Plate Reader, using BeyoGold™ 96-Well Black Opaque plates. The excitation wavelength for compound A1 was set at 399 nm. To analyze the viscosity effects, a graph was plotted with the logarithm of solvent viscosity on the x-axis and the logarithm of emission intensity on the y-axis. The viscosity dependence factor, represented by ' *x* ', was calculated using the Förster-Hoffmann equation (Equation S2).

$$\log I = x\log \eta + c \quad \text{(S2)}$$

in which *I* is the fluorescence intensity, *η* is viscosity, *x* is the viscosity sensitivity, *C* is a constant and *x* represents the sensitivity of the fluorescent probe to the viscosity. Error bar: standard error (n = 3).

1.5 Plasmids construction and protein purifications

E. coli wild type DHFR (WT-DHFR), mutant-DHFR (M42T: H114R) and sortase genes were codon optimized, synthesized, and sub-cloned into pET- 29b (+) vectors. To facilitate purification, all proteins were cloned with His-tag at the C-termini. Wild type TTR (WT-TTR) genes were codon optimized, synthesized by GenScript in Nanjing, China, and sub-cloned into pET-29b (+) vectors without His-tag to minimize amyloid formation interference. Human serum albumin (HSA) was purchased from CSL Behring AG.

BL21(DE3) *E. coli* cells were transformed with WT-DHFR, mut-DHFR (M42T: H114R),

and sortase protein plasmids. Cells were grown to OD_{600} of 0.6-0.8 before being stimulated by IPTG (0.5 mM) at 37 °C for 4 h (WT-DHFR), 30 °C for 4 h (mut-DHFR (M42T: H114R)), 18 °C for 16 h (sortase). Cultured cells were resuspended in resuspension buffer (50 mM Tris•HCl, 100 mM NaCl, pH = 8.00). Cells expressing recombinant proteins were thawed and lysed by sonication at 4 °C. Lysed cells were centrifuged at 12,000 rpm for 30 min. The supernatant was collected and loaded onto a 10 mL Ni-NTA column, which was then washed with buffer (50 mM Tris•HCl, 100 mM NaCl, pH = 8.00). Proteins were then eluted by gradient increase of imidazole buffer (50 mM Tris·HCl, 100 mM NaCl, 500 mM imidazole, pH = 8.00). The protein fractions were identified by SDS-PAGE analysis, pooled, and concentrated. Proteins purified by Ni-NTA column were further purified using 120 mL Superdex 200 size-exclusion column in phosphate buffer (10 mM sodium phosphates, 100 mM KCl, 1 mM EDTA, acidified by HCl to pH = 7.40). Fractions containing target proteins were identified by SDS-PAGE gel analysis, pooled, and concentrated. Based on SDS-PAGE gel, the purity was estimated at > 95% with no significant impurities identified.

WT-TTR was expressed in E. coli BL21 DE3 cells and purified using a 4-step method including a salt-cut step and three chromatographic steps described in previous publication. A pET29b (+) vector encoding the TTR-L55P sequence was transformed into BL21 DE3 cells and plated onto LB-agar plates with kanamycin. When cell growth monitored by OD600 reached 0.6-0.8, isopropyl β-D-1-thiogalactopyranoside (IPTG, 1 mM) was introduced into culture to induce the overexpression of WT-TTR, and after induction of 5 h, the cells were harvested by centrifugation (10 min at 13700 × g). WT-TTR was purified at room temperature. Fresh cell pellets were re-suspended in Buffer A (50 mM Tris, 150 mM NaCl, pH 7.5; 15 mL buffer/L of culture). Re-suspended cells were thawed and lysed by sonication at 4 °C. The sonication was carried out using 80% of the output power on a mode with 2 seconds on and 2 seconds off for 1 min. This process was repeated 6 times. Lysed cell suspension was centrifuged for 30 min at 16,000 × g and supernatant were collected for following step. To precipitate the majority of the cellular proteins, ammonium sulfate (242 $g \cdot L^{-1}$) was slowly added into the supernatant with rigorous stirring at 4 °C for 15 min. The solution was then centrifuged at 12,000 × g for 15 min at 4 °C. The pellet (mostly proteins other than WT-TTR) was discarded, and the supernatant containing WT-TTR was supplemented with additional ammonium sulfate to a final concentration of 365 $g \cdot L^{-1}$ with rigorous stirring at 4 °C for 15 min. The solution was centrifuged at 12,000 × g for another 15 min at 4 °C. The pellet was resuspended in 20−30 mL of anion exchange buffer A (25 mM Tris and 1 mM EDTA, pH 8.0) and dialyzed against 4 L of buffer A at 4 °C overnight. After dialysis, the protein solution was filtered through 0.45 μm film and purified by 50 mL Source 15Q anion exchange column equilibrated with buffer A. WT-TTR was eluted using a linear gradient of NaCl (160 mL; 50−350mM) followed by a NaCl wash (50 mL, 350 mM). Fractions containing WT-TTR was further purified using a 120 mL Superdex 75 gel filtration column in SEC buffer (10 mM sodium phosphate, 100 mM KCl, and 1 mM EDTA, pH = 7.6) to remove contaminants and other soluble aggregates. The above steps together yielded WT-TTR in SEC buffer. Based on SDS-PAGE gel, the purity was estimated > 98% without significant impurities identified.

1.6 Detection linear range and lowest limit of detection

For measurements of linear range and the limit of detection (LOD), freshly

prepared WT-DHFR in phosphate buffer (10 mM phosphate, 100 mM KCl, 1 mM EDTA, acidified by concentrated HCl to pH = 7.40) was diluted to 50 μM with acidic aggregation buffer (NaOAc 200 mM, KCl 100 mM, acidified by AcOH to pH = 6.23) and mixed with different concentration of A1 (0.1-50 μM). The samples were incubated at 65 °C for 5 min for fully aggregating WT-DHFR. Fluorescence intensity was recorded by exciting the samples at 399 nm and collecting the max fluorescent intensity. Error bars: standard error (n = 3). The concentration-dependent fluorescence intensity of A1 showed linearity in the range of 0.1-20 μM. The lowest limit of detection was down to 0.1 μM

1.7 Fractionation experiment of aggregated DHFR

A mixture of WT-DHFR at a concentration of 50 μM and either A1 at 15 μM was prepared in an aggregation buffer (200 mM NaOAc, 100 mM KCl, adjusted to pH 6.23 with AcOH). This mixture was heated at 65 °C for 5 minutes. Six replicates of 120 μL each were set up. After ensuring full protein aggregation, 100 μL from three of these samples (designated as total aggregated, T) was used for fluorescence measurements, while the remainder was saved for electrophoresis. The other three samples underwent centrifugation at 4 °C for 15 minutes to separate into soluble supernatant (S) and insoluble precipitate (I). The insoluble fraction was resuspended in an equal volume of aggregation buffer after the soluble fraction was carefully removed and set aside for fluorescence and electrophoresis studies.

(1) For fluorescence readings, 100 μL of the total aggregated sample (T), the soluble supernatant (S), and the resuspended insoluble precipitate (I) were pipetted into BeyoGold 96-Well Black Opaque plates. A Tecan Spark Fluorescence Plate Reader was used with a 399 nm excitation wavelength to measure the fluorescence emission intensity. The standard error was calculated with three replicates (n=3). (2) Additionally, fluorescence imaging of these fractions was performed under UV light at 365 nm.

1.8 Thermal shift assay to quantitatively analyze protein thermodynamic stability.

Thermal shift assay by OD_{330}:

Freshly purified WT-DHFR protein in acidic aggregation buffer (200 mM NaOAc, 100 mM KCl, acidified by AcOH to pH = 6.23) under different temperatures for 5 min. The incubated mixture was pipetted into quartz cuvette to measure optical density at 330 nm (OD_{330}).

Thermal shift assay by A1:

Freshly purified WT-DHFR protein (50 μM) and A1 (5 μM) were mixed in acidic aggregation buffer (200 mM NaOAc, 100 mM KCl, acidified by AcOH to pH = 6.23) and incubated from 25 °C to 65 °C for 5 min. The incubated mixture (100 μL) was transferred into a BeyoGold96-Well Black Opaque plates to collect fluorescence emission intensity using Tecan Spark Fluorescence Plate Reader. Exci- 1tation wavelength was 399 nm for A1. Error bars: standard error (n = 3).

The melting temperatures (T_m) were obtained through non-linear curve fitting of optical density readings at different incubation temperatures using the program OriginPro 2018:

$$F(T) = F(post) + \frac{[F(pre) - F(post)]}{1 + exp\{\frac{-\triangle H_u}{R}\left(\frac{1}{T} - \frac{1}{T_m}\right) + \frac{\triangle C_{pu}}{R}\left[\ln\left(\frac{T}{T_m}\right) + \frac{T}{T_m} - 1\right]\}}$$

in which F(T) is the OD_{330} signal at temperature T; T_m is the melting temperature of the protein aggregation transition, F(pre) and F(post) are the initial and ending transitional OD_{330} signal, respectively, R is the gas constant, ΔH_u is the enthalpy of protein aggregation, and ΔC_{pu} is the heat capacity change upon protein aggregation.

1.9 Proteolytic resistance.

To measure the fluorescence decrease kinetics profile upon proteolysis, proteinase K (50 μg·mL^{-1}) was introduced to 120 μL aggregated protein solution (50 μM WT-DHFR, 5 μM A1). The reaction mixture was incubated at room temperature for indicated time. The suspension was centrifuged and the supernatant was aspirated, then equal volume of aggregation buffer (200 mM NaOAc, 100 mM KCl, acidified by AcOH to pH = 6.23) was added to resuspend. Fluorescent spectra were collected from 0 min to 90 min with 5-min intervals.

1.10 Aggregation conditions for different recombinant proteins

For WT-DHFR, mutant-DHFR (M42T:H114R), sortase, Lysate (E. coli) and human serum albumin (HSA):

In a specially prepared acidic aggregation buffer (200 mM NaOAc, 100 mM KCl, pH adjusted to 6.23 with AcOH), a freshly purified protein at 50 μM was combined with either A1 at a 15 μM concentration. The mixture was then heat-treated for 5 minutes at varying temperatures depending on the type of protein (65 °C for WT-DHFR, E. coli lysate, and mutant-DHFR; 70 °C for sortase; 95 °C for human immunoglobulin). Following incubation, 100 μL of the homogenized solution was transferred into BeyoGold™ 96-Well Black Opaque plates. Fluorescence measurements were taken using a Tecan Spark Fluorescence Plate Reader with an excitation wavelength of 399 nm for A1. Error bars represent the standard error based on three replicates (n=3).

For WT-TTR:

In acidic aggregation buffer (NaOAc 200 mM, KCl 100 mM, acidified by AcOH to pH = 4.4), freshly purified WT-TTR (3.6 μM) and A1 probe (15 μM) were mixed and incubated at 95 °C for 10 min. The incubated mixture (100 μL) was pipetted into BeyoGold™ 96-Well Black Opaque plates to collect fluorescence emission using Tecan Spark Fluorescence Plate Reader. Excitation wavelength was 399 nm for A1 . Error bars: standard error (n = 3).

1.11 CCK8 assay for A1.

TU212 cell (laryngeal carcinoma cell) were cultured in IMDM medium supplemented with 10% FBS and 1% antibiotics (penicillin-streptomycin), and maintained at 37°C in a 5% CO2 humidified atmosphere. Upon reaching 60% confluency, the cells were transferred to 96-well plates at a density of 10,000 cells per well in 200 μL of the medium. The culture medium was then swapped out for

fresh IMDM containing varying levels of probe A1 and incubated for an additional 24 hours. Following this period, the medium was changed to 100 µL of fresh IMDM, which contained 10% CCK-8, and the cells were incubated for another hour in the dark. Absorbance readings were subsequently taken at 450 nm using a Tecan Spark Fluorescence Plate Reader. A control group was also maintained, following the same procedures but without the addition of any fluorescent probes. Finally, relative cell viability was determined using the formula: Cell Viability (%) = (OD_{sample} - $OD_{background}$) / ($OD_{control}$ - $OD_{background}$) × 100%.

1.12 Confocal imaging of aggregated proteome in stressed cells

TU212 cells were cultured in IMDM medium enriched with 10% FBS and 1% Penicillin-Streptomycin and were allowed to grow until they reached 70% confluency in 20 mm NEST glass-bottom dishes that were sterile and non-pyrogenic. Twelve hours before the experiment, the cells were seeded to achieve 70% confluency.

For the experimental group, both 0.5 M sorbitol and either A1 at a concentration of 5 µM were added to the medium, followed by a 10-minute incubation. The medium was then replaced with fresh A1 containing Hoechst 33342 and left to incubate for another 30 minutes.

For the negative control, either A1 at 5 µM was added to the cells and incubated for 10 minutes. This was followed by a medium replacement and a further 30-minute incubation.

Fluorescence images were captured using an Olympus FV1000 FluoView™ confocal microscope. Nuclear staining was visualized with a green laser at 488nm, while the fluorescence from the aggregated proteome in the cellular environment was observed using an UV laser at 405 nm.

1.13 Confocal λ-imaging and quantitative image analysis

Cell culture for λ-imaging followed the same as above-mentioned method. For A1 λ-deconvolution: Excitation wavelength was 405 nm, and emission spectra were collected in 460 nm – 520 nm with a 2 nm step-size and 5 nm band width. Images were collected using Olympus FV1000MPE.

1.14 Histological analysis of laryngeal carcinoma tissue sections with different degrees of hepatic stress.

Fresh laryngeal carcinoma tissue samples were encased in an optimal cutting temperature (OCT) compound and then sliced into 6 µm thick sections using an EICA CM1950 clinical cryostat. These sections were then stabilized in chilled acetone at 4°C for a span of 10 minutes and stored at -20°C for later use. When required, these stored sections were gradually thawed, first at 4°C and then at room temperature, each for 30 minutes. Post-thawing, the sections were rinsed thrice in PBS buffer, each rinse lasting 5 minutes. PAP pen was used to outline the target areas on the tissue, which were then treated with A1 solutions at a concentration of 5.0 µM. This was followed by a dark incubation for 1 hour and a brief 5-minute soak in PBS buffer. For additional staining, sections were treated with SYTO9 Nucleic Acid Stains at a 2.0 µM concentration for 15 minutes and then rinsed in PBS. The sections were then sealed with an anti-fade mounting medium. Fluorescence

images were captured using an Olympus FV1000 FluoView™ confocal microscope. The nuclear staining was visualized using a 488 nm green laser, while aggregated proteomes in the target tissue areas that were marked with the A1 probe were observed under a 405 nm violet laser.

1.15 Confocal λ-imaging and quantitative image analysis

Preparation of tissue sections for λ-imaging followed the same operation as above-mentioned **1.13** method. For A1 λ-deconvolution: Excitation wavelength was 405 nm, and emission spectra were collected in 460 nm – 520 nm with a 2 nm step-size and 5 nm band width. Images were collected using Olympus FV1000MPE.

2. Supplementary Figures

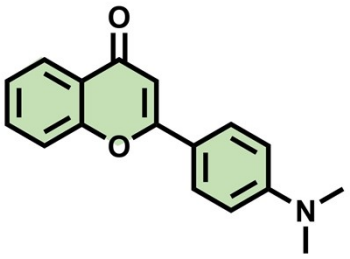

A1

	solvent	dielectric constant	λ_{abs} (nm)	λ_{em} (nm)	$\Delta\lambda$ (nm)
1	Glycerol	46.50	399	519	120
2	Glycol	37.00	393	523	130
3	MeOH	32.70	384	518	134
4	EtOH	24.50	383	506	123
5	i-PrOH	19.90	379	489	110
6	n-BuOH	17.10	381	492	111
7	t-BuOH	11.40	376	475	99
8	DCM	8.90	373	458	85
9	THF	7.60	367	449	82
10	Ethyl Acetate	6.02	360	451	91
11	Toluene	2.40	364	439	75
12	Dioxane	2.25	363	439	76

Figure S1. Photophysical properties of A1 across different solvents. All measurements were carried out using Tecan Spark Fluorescence Plate Reader in NEST 96-Well flat bottom transparent plates. Measurements in different solvents were described in **Experimental Methods 1.2**. All measurements were repeated for three times.

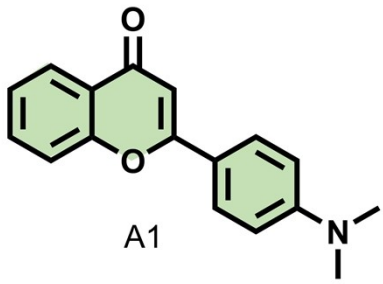
O
O
N
A1

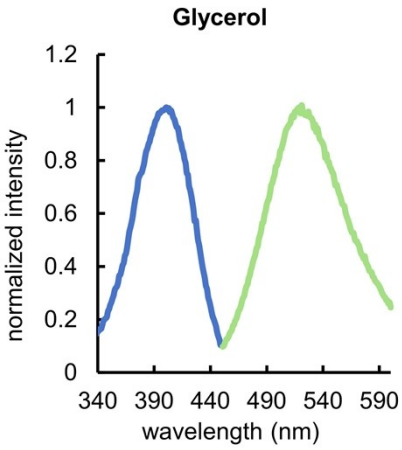
Glycerol
normalized intensity
1.2
1
0.8
0.6
0.4
0.2
0
340 390 440 490 540 590
wavelength (nm)

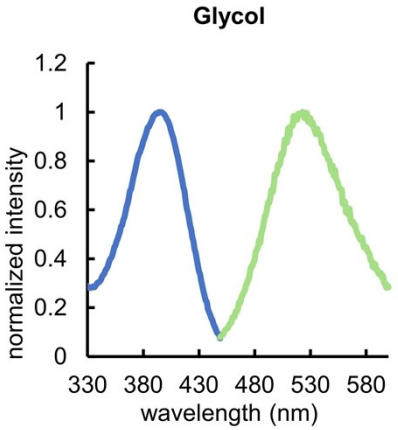
Glycol
normalized intensity
1.2
1
0.8
0.6
0.4
0.2
0
330 380 430 480 530 580
wavelength (nm)

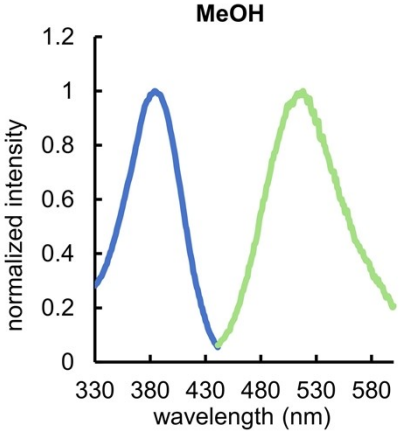
MeOH
normalized intensity
1.2
1
0.8
0.6
0.4
0.2
0
330 380 430 480 530 580
wavelength (nm)

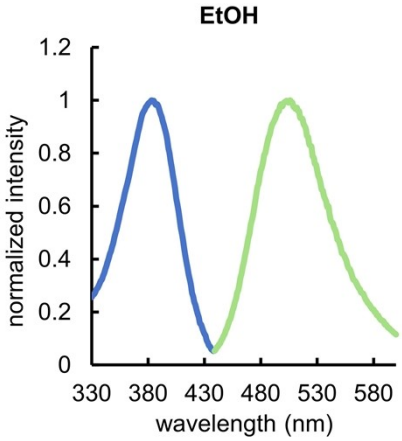
EtOH
normalized intensity
1.2
1
0.8
0.6
0.4
0.2
0
330 380 430 480 530 580
wavelength (nm)

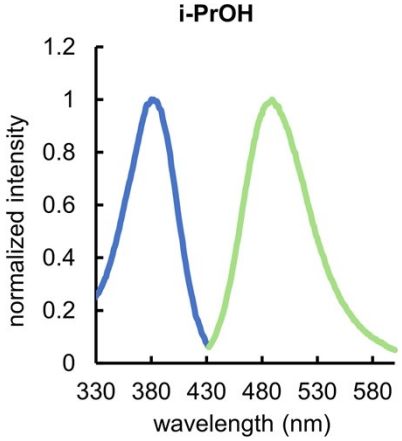
i-PrOH
normalized intensity
1.2
1
0.8
0.6
0.4
0.2
0
330 380 430 480 530 580
wavelength (nm)

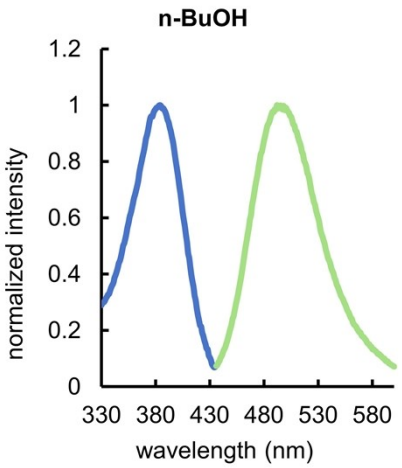
n-BuOH
normalized intensity
1.2
1
0.8
0.6
0.4
0.2
0
330 380 430 480 530 580
wavelength (nm)

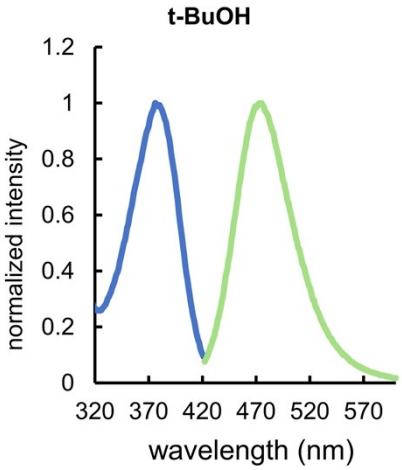
t-BuOH
normalized intensity
1.2
1
0.8
0.6
0.4
0.2
0
320 370 420 470 520 570
wavelength (nm)

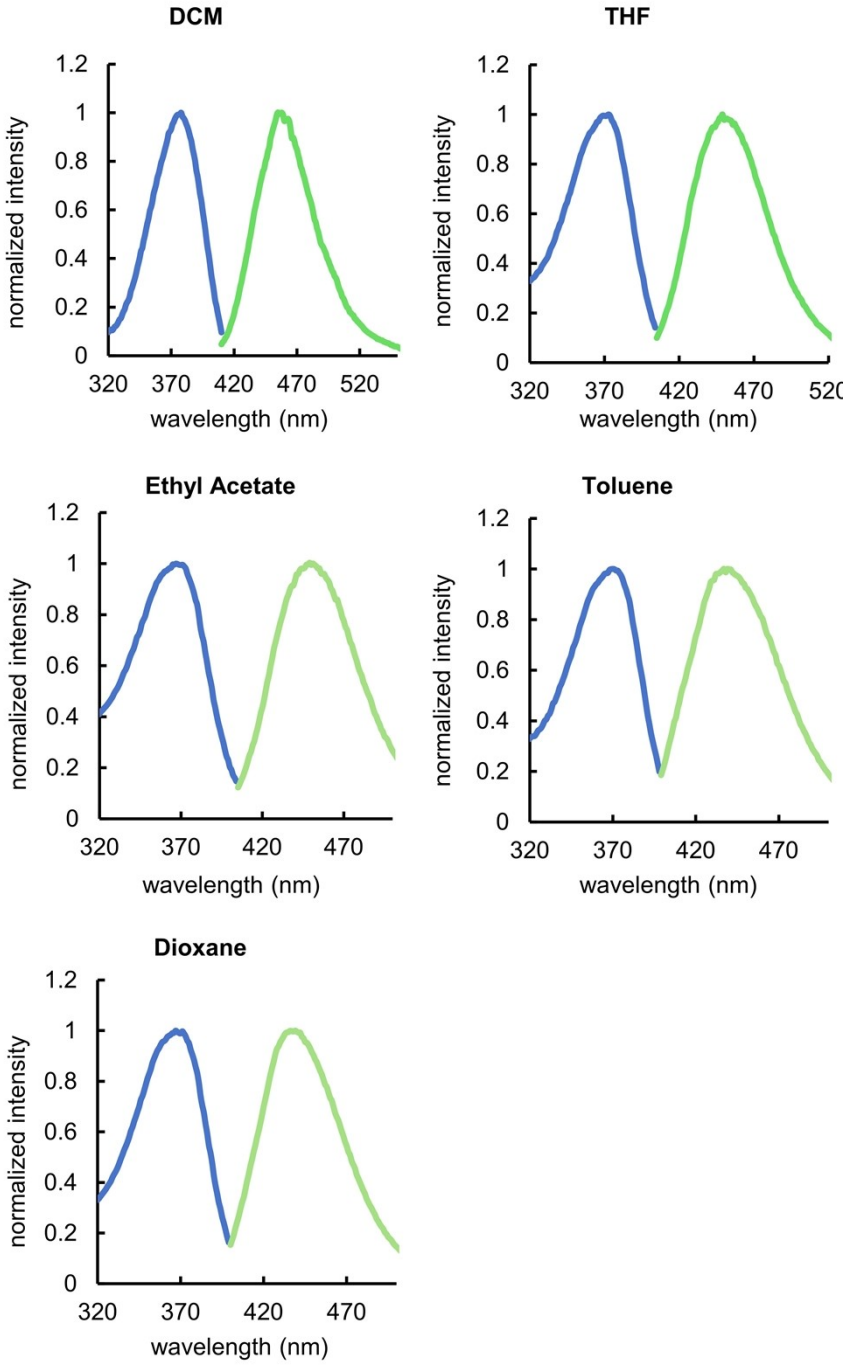

Figure S2. Normalized fluorescence excitation and emission spectra of A1 across the tested solvents. A1 was prepared to 20 μM for excitation scan and emission measurements. All measurements were carried out using Tecan Spark Fluorescence Plate Reader in NEST 96-Well flat bottom transparent plates. The experimental procedure followed **Experimental Methods 1.2**. All measurements were repeated for three times.

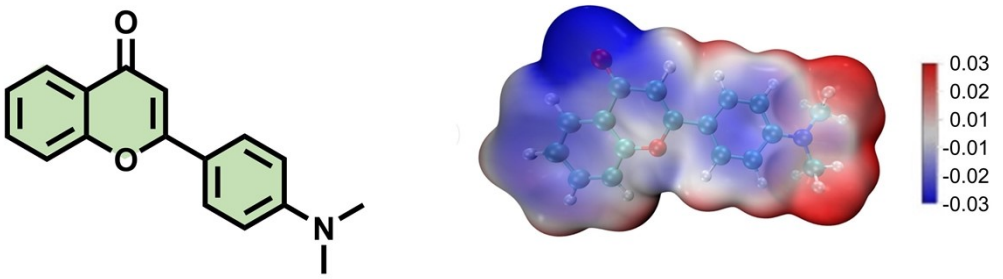

Figure S3. The charge separation of polar A1 molecules allows the presence of intramolecular charge separation. Electrostatic potential maps based on the electron density of A1, indicating the charge separation inside molecules.

(a)

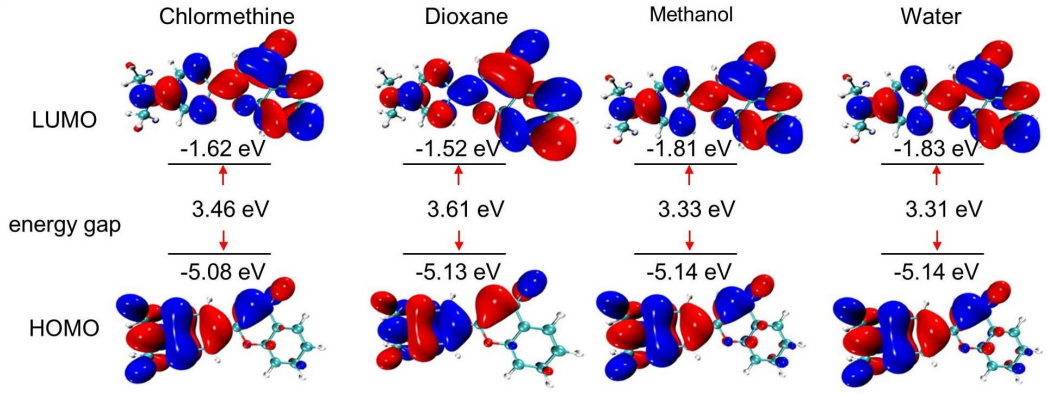

(b)

Solvent	Excited states	Configuration	Oscillator strength	Energy (eV/nm)
chlormethine	S1	70 → 71 HOMO → LUMO	1.08	3.01 (411.36)
dioxane	S1	70 → 71 HOMO → LUMO	0.81	3.25 (381.53)
methanol	S1	70 → 71 HOMO → LUMO	1.12	2.85 (435.74)
water	S1	70 → 71 HOMO → LUMO	1.13	2.82 (440.07)

Figure S4. Twisted intramolecular charge transfer (TICT) state variations of Probe A1 in different solvents. (a) The electronic cloud distribution diagrams of the frontier molecular orbitals and energies at the excited S1 state of probe A1 in various solvents, along with their corresponding energy level differences. (b) Under different solvent conditions, the characteristics of the excited-state electronic transitions of probe A1, including oscillator strengths, energy gaps between the excited and ground states, and the wavelengths of the emission spectra. The experiment was conducted in accordance with **Experimental Methods section 1.3**

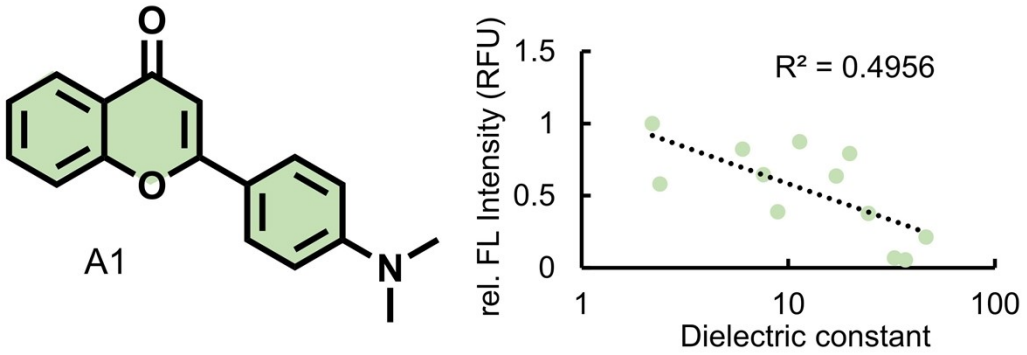

Figure S5. The relative fluorescence emission intensity of A1 in solvents bearing different dielectric constant. Compared to the emission wavelength versus dielectric constant in **Fig. 2**, the emission intensity of A1 displayed no obvious correlation with dielectric constant.

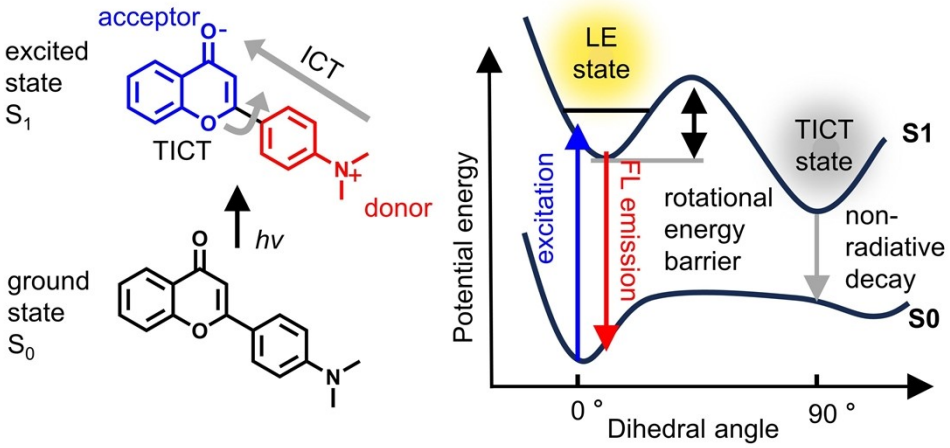

Figure S6. The solvatochromic probe A1 underwent a transition from the ground state to the excited state, potentially involving an intramolecular charge transfer process. While initially in its ground state (S_0), the molecule was elevated to an excited state (S_1) upon photon excitation. In this excited state, intramolecular charge transfer (ICT) could occur. At this point, the molecule transitioned from its initial locally excited (LE) state to a twisted intramolecular charge transfer (TICT) state.

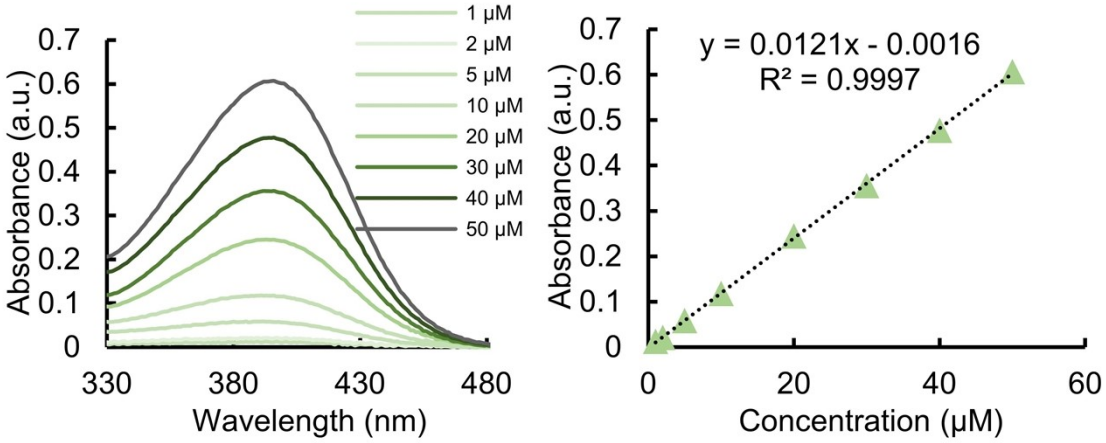

Figure S7. The linear range of A1 in DMSO. The A1 was diluted from 1mM stock solution to prepare different concentrations in PBS buffer. A1 exhibited linear range up to 50 μM in aqueous condition.

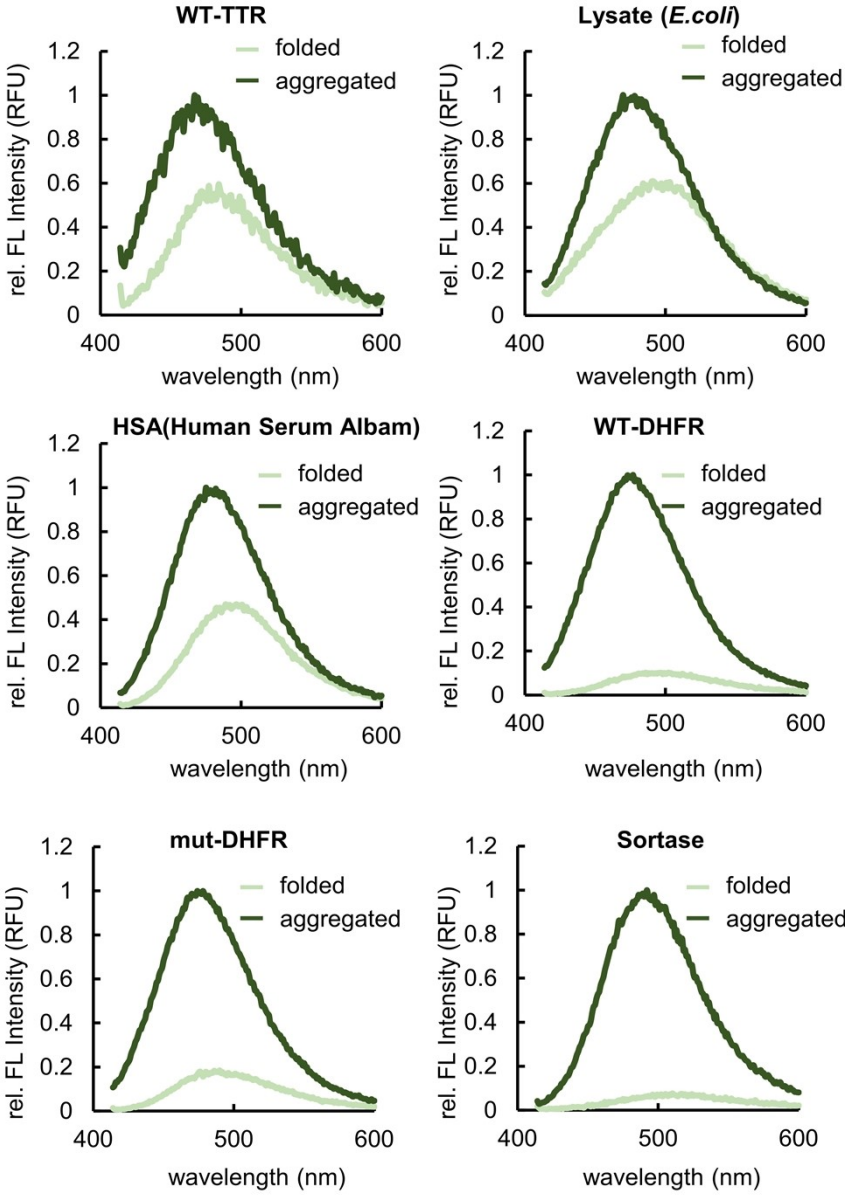

protein	wavelength	ε
WT-TTR	467	8.06
Lysate(E.coli)	470	8.89
HAS	475	10.47
WT-DHFR	477	11.18
mut-DHFR	478	11.55
Sortase	492	18.27

Figure S8. Emission spectra of the solvatochromic probe A1 correspond to different protein conformations, both in the folded and aggregated states. A1 could detecting the aggregation processes across a diverse range of protein types and allows for the

quantification of microenvironmental polarity changes that transpire during aggregation.

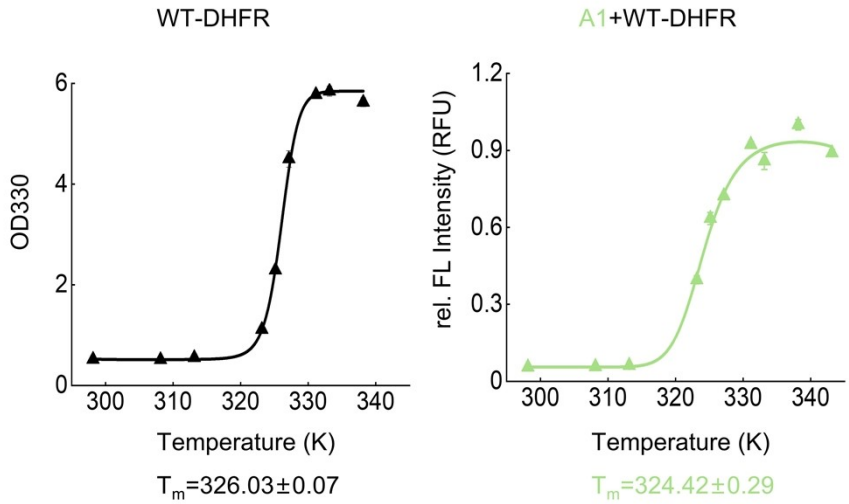

Figure S9. Thermal shift analysis emphasizes that the fluorescence of A1 occurs at lower temperature than the OD330 turbidity signal which measures the aggregation process of WT-DHFR. The experimental procedure followed **Experimental Methods 1.8**

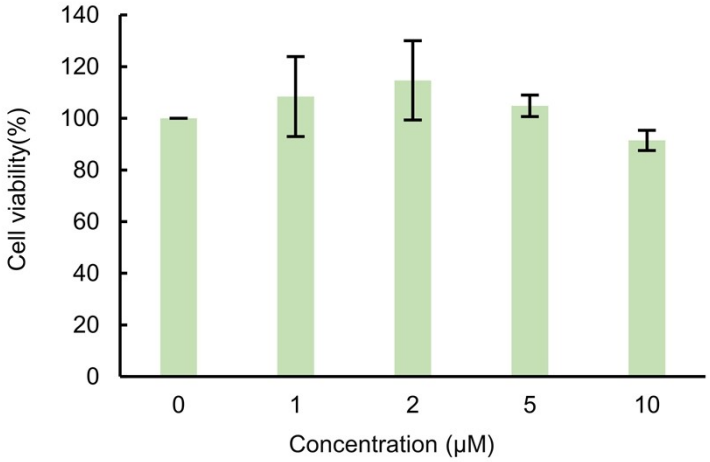

Figure S10. A1 exhibit negligible cytotoxicity in TU212 cells up to 10 μM concentration. The experiment was conducted in accordance with **Experimental Methods section 1.11**

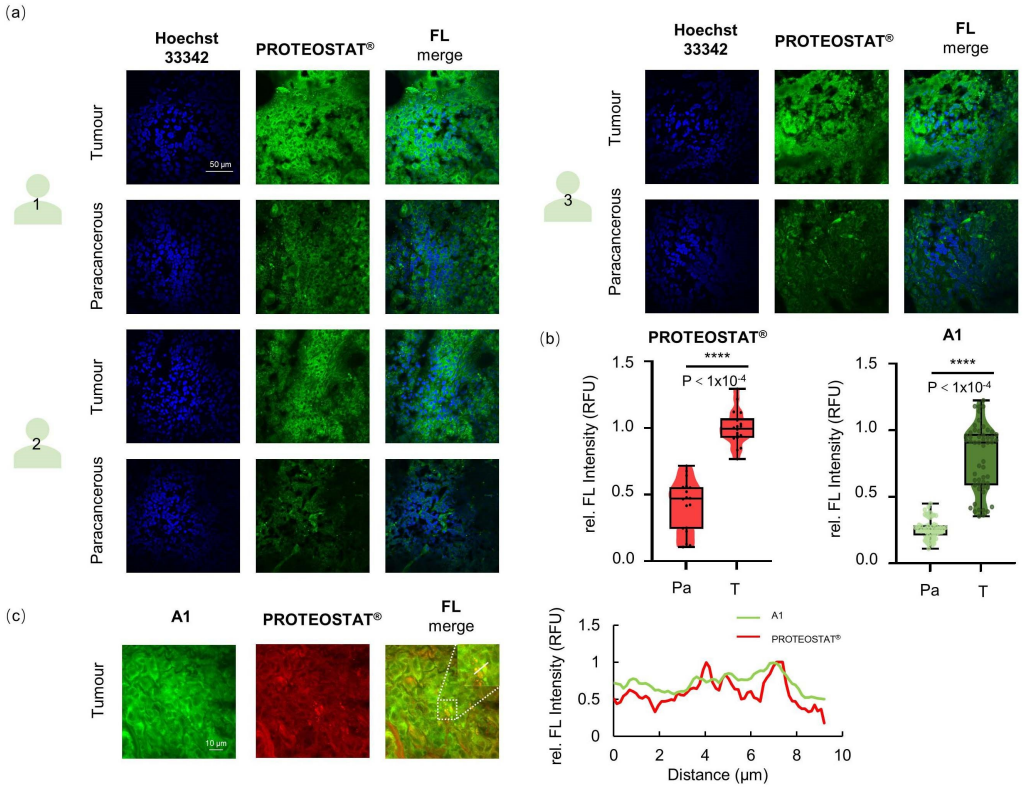

Figure S11. Protein aggregation in cancer tissues leads to enhanced fluorescence intensity of probe A1 in laryngeal cancer tissues. (a) Staining of laryngeal cancer and paracancerous tissues using the commercial PROTEOSTAT® Aggresome Detection Kit reveals an increase in aggregated proteins in laryngeal cancer tissues compared to paracancerous tissues. (b) A comparison of the fluorescence intensity between PROTEOSTAT dye and Probe A1 in laryngeal cancer and paracancerous tissues shows higher fluorescence intensity in the tumor tissues. (c) Co-localization of PROTEOSTAT dye and Probe A1 in laryngeal cancer tissues.

3. References

1. Wan, W.; Zeng, L.; Jin, W.; Chen, X.; Shen, D.; Huang, Y.; Wang, M.; Bai, Y.; Lyu, H.; Dong, X.; Gao, Z.; Wang, L.; Liu, X.; Liu, Y., A Solvatochromic Fluorescent Probe Reveals Polarity Heterogeneity upon Protein Aggregation in Cells. *Angewandte Chemie International Edition* **2021,** *60* (49), 25865-25871.

2. Gaussian 16 Rev. B.01, (2016), M.J. Frisch, G.W. Trucks, H.B. Schlegel, G.E. Scuseria, M.A. Robb, J.R. Cheeseman, G. Scalmani, V. Barone, G.A. Petersson, H. Nakatsuji, X. Li, M. Caricato, A.V. Marenich, J. Bloino, B.G. Janesko, R. Gomperts, B. Mennucci, H.P. Hratchian, J.V. Ortiz, A.F. Izmaylov, J.L. Sonnenberg, Williams, F. Ding, F. Lipparini, F. Egidi, J. Goings, B. Peng, A. Petrone, T. Henderson, D. Ranasinghe, V.G. Zakrzewski, J. Gao, N. Rega, G. Zheng, W. Liang, M. Hada, M. Ehara, K. Toyota, R. Fukuda, J. Hasegawa, M. Ishida, T. Nakajima, Y. Honda, O. Kitao, H. Nakai, T. Vreven, K. Throssell, J.A. Montgomery Jr., J.E. Peralta, F. Ogliaro, M.J. Bearpark, J.J. Heyd, E.N. Brothers, K.N. Kudin, V.N. Staroverov, T.A. Keith, R. Kobayashi, J. Normand, K. Raghavachari, A.P. Rendell, J.C. Burant, S.S. Iyengar, J. Tomasi, M. Cossi, J.M. Millam, M. Klene, C. Adamo, R. Cammi, J.W. Ochterski, R.L. Martin, K. Morokuma, O. Farkas, J.B. Foresman and D.J. Fox, D.J. Gaussian, Inc., Wallingford CT (2016) GaussView 5.0. Wallingford, E.U.A.

3. Qian, H.; Cousins, M. E.; Horak, E. H.; Wakefield, A.; Liptak, M. D.; Aprahamian, I., Suppression of Kasha's rule as a mechanism for fluorescent molecular rotors and aggregation-induced emission. *Nature Chemistry* **2017,** *9* (1), 83-87.